

Design, Synthesis, and Biological Action of 20*R*-Hydroxyvitamin D3Yan Lu,<sup>†</sup> Jianjun Chen,<sup>†</sup> Zorica Janjetovic,<sup>‡</sup> Phillip Michaels,<sup>‡</sup> Edith K. Y. Tang,<sup>§</sup> Jin Wang,<sup>†</sup> Robert C. Tuckey,<sup>§</sup> Andrzej T. Slominski,<sup>‡</sup> Wei Li,<sup>\*,†</sup> and Duane D. Miller<sup>\*,†</sup><sup>†</sup>Department of Pharmaceutical Sciences, University of Tennessee Health Science Center, Memphis, Tennessee 38163, United States<sup>‡</sup>Department of Pathology and Laboratory Medicine, Center for Cancer Research, and Department of Medicine, Division of Dermatology, University of Tennessee Health Science Center, Memphis, Tennessee 38163, United States<sup>§</sup>School of Biomedical, Biomolecular and Chemical Sciences, University of Western Australia, Crawley, WA, Australia

## Supporting Information

**ABSTRACT:** The non-naturally occurring 20*R* epimer of 20-hydroxyvitamin D3 is synthesized based on chemical design and hypothesis. The 20*R* isomer is separated by semipreparative HPLC, and its structure is characterized. A comparison of 20*R* isomer to its 20*S* counterpart in biological evaluation demonstrates that they have different behaviors in antiproliferative and metabolic studies.

## INTRODUCTION

Vitamin D hormone carries out essential biological functions required for human health. Besides its critical role in regulating bone formation and calcium homeostasis, vitamin D hormone also regulates cell growth, differentiation, proliferation, apoptosis, and immune responses through the activation of the nuclear vitamin D receptor (VDR).<sup>1,2</sup> Vitamin D3 is derived from a cholesterol precursor in the skin, 7-dehydrocholesterol (7-DHC). After absorption of ultraviolet B (UVB) radiation (315–280 nm wavelength), 7-DHC is converted to previtamin D3, which undergoes further thermally induced transformation to vitamin D3 (cholecalciferol). Vitamin D3 from the diet or produced in the epidermis is biologically inactive and requires enzymatic conversion to 1,25-dihydroxyvitamin D3 (1,25(OH)<sub>2</sub>D3, calcitriol), the active form of vitamin D3. This activation involves sequential 25- and 1 $\alpha$ -hydroxylation in the liver and kidney, respectively.<sup>3</sup> Unfortunately, the toxicity (hypercalcemia) induced by high levels of vitamin D largely prevents the clinical use of pharmacological doses of 1,25(OH)<sub>2</sub>D3. More than 40 metabolites of vitamin D have been reported,<sup>4</sup> and understanding the activity of these metabolites can assist in the development of new vitamin D3 analogues with beneficial actions. Searching for vitamin D analogues that retain biological efficacy and display minimal or no hypercalcemia has been pursued for several decades. As a result, several vitamin D analogues that exhibit reduced hypercalcemia are entering clinical trials and are showing great promise as potential therapeutic agents for the treatment of cancer and other diseases.<sup>5</sup>

20*S*-Hydroxyvitamin D3 (20*S*(OH)D3, Figure 1) is a newly isolated metabolite of vitamin D3 produced by the action of the enzyme cytochrome P450<sub>scc</sub> (CYP11A1).<sup>6,7</sup> It inhibits cell proliferation and differentiation without inducing hypercalcemia at a dose of 30  $\mu$ g/kg on mice (unpublished results), stimulates VDR gene expression, and inhibits NF $\kappa$ B activity with similar potency to 1,25(OH)<sub>2</sub>D3.<sup>8</sup> We have chemically synthesized 20*S*(OH)D3,<sup>6b</sup> which exhibited biological proper-

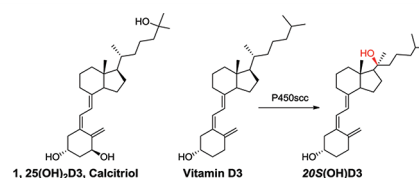


**Figure 1.** Structures of calcitriol, vitamin D3, and new VD3 metabolite 20*S*(OH)D3.

ties similar to those of 20*S*(OH)D3 generated enzymatically using P450<sub>scc</sub>. The *S* configuration of C-20 in chemically synthesized 20*S*(OH)D3 was determined by NMR and HPLC and was found to be identical to the enzymatically generated metabolite. Many reported potent D3 analogues have 21 $\beta$ -Me configuration which corresponds to the 20*R*(OH)D3 configuration.<sup>9</sup> These analogues are very potent VDR activators with very low hypercalcemic side effect.<sup>10</sup> It will be very interesting to see if 20*R*(OH)D3 has different activity compared with 20*S*(OH)D3. Hansen et al. have reported the preparation of 20*R*(OH)D3 analogues with 22-alkynyl side chains from secosteroids.<sup>11</sup> In this report, we designed an efficient synthetic route to prepare 20*R*(OH)-7DHC from pregnenolone, which after UVB irradiation and HPLC purification yielded the 20*R*(OH)D3 epimer. Analysis of its NMR spectra and comparison to that of 20*S*(OH)D3 confirmed the formation of the 20*R*-epimer without detectable amounts of the other.

A noticeable phenomenon was reported in the preparation of 20*S*(OH)-7DHC that only 20*S* epimer was produced from the Grignard reaction, while theoretically 20*R*- and 20*S*(OH)-7DHC should be obtained. This result suggested that the attack of Grignard agent is highly stereoselective at the 20-cabonyl position (Figure 2). A similar phenomenon was also reported in the synthesis of 20*S*-hydroxycholesterol and other 20-hydroxysteroids.<sup>12</sup> Theoretical calculation and NMR spectra characterization<sup>6b</sup> of synthesized 20*S*(OH)-7DHC clearly

Received: November 11, 2011

Published: March 9, 2012

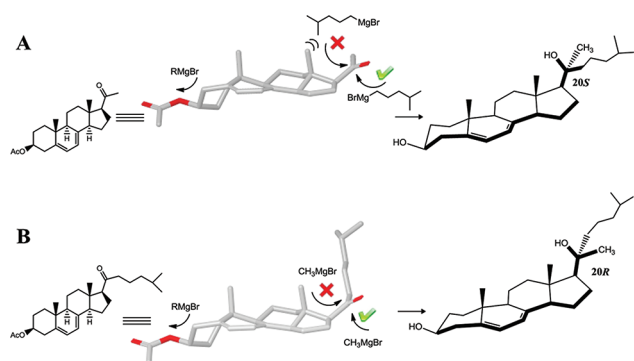


**Figure 2.** Hypothesis to obtain 20R-epimer. Molecular models were constructed using the MM2 energy minimization algorithm in ChemBioOffice 2010 Chem 3D Pro (version 12.0). (A) It was proved that “bottom” side attack by the bulky Grignard reagent to form the 20S epimer is favored while attack from the “top” is prohibited because of the steric hindrance from 18-CH<sub>3</sub> and the steroid scaffold. (B) We hypothesize that “bottom” side attack of the small sized CH<sub>3</sub>MgI is favored by the pre-existing bulky side chain while it is not inclined to attack from “top” side to form the 20R epimer.

indicate that there is a preference for the orientation of the 17-acetyl group. It is conceivable that this conformational preference dictated the outcome of the bulky side chain addition to form 20S epimer. As shown in Figure 2A, the attack of the nucleophilic Grignard reagent takes place predominantly from the less hindered “bottom” side of the carbonyl group to form 20S(OH)-7DHC while the attack from the “top” side to form 20R(OH)-7DHC is sterically prohibited.

The above observations encourage us to design a synthesis approach to exclusively produce 20R(OH)-7DHC. We predict that if the bulky side chain at the 20-carbonyl position is introduced in earlier synthesis steps, followed by introducing the 21-methyl group with smaller Grignard reagent CH<sub>3</sub>MgI, the 20R conformation should be obtained as the only epimer product (Figure 2B). To validate our hypothesis, we employed chemical synthesis to access material for biological evaluation. The synthesis route of 20R(OH)D3 is shown in Scheme 1.

## RESULTS AND DISCUSSION

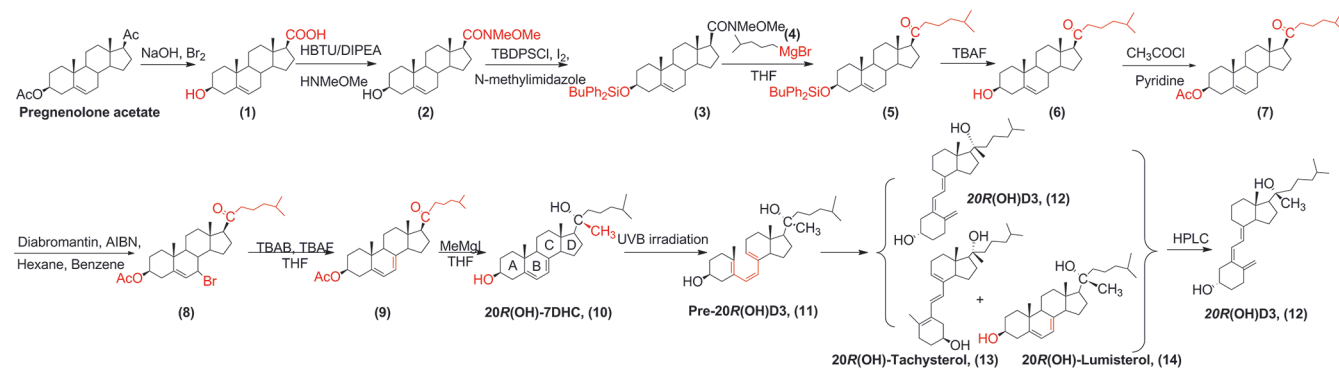
**Chemistry.** The synthesis of 20R(OH)-7DHC started with high yield (>95%) conversion of pregnenolone acetate to 3 $\beta$ -acetoxyetentic acid **1** under oxidation with in situ prepared NaOBr from bromine and sodium hydroxide solution.<sup>13</sup> We tried the coupling conditions employing EDCI/HOBt/NMM

to introduce Weinreb amide, but the major product separated was the intermediate active ester of benzotriazolyl carboxylate, which is close to the desired **2** on the TLC plate but showed UV absorption. We therefore changed coupling conditions to HBTU/DIPEA/HNMeOMe·HCl salt which was reacted with 17 $\alpha$  carboxylic acid to yield Weinreb amide in 75.9% yield. We chose introducing silicon ether protection of the 3 $\beta$ -hydroxyl in the next step to reduce the consumption of (4-methylpentyl) magnesium bromide **4**, which was prepared from 1-bromo-4-methylpentane and magnesium turnings in anhydrous THF. Three silyl chlorides (TMSCl, TBDMSCl, and TBDPSCl) were used in the presence of various bases such as triethylamine, imidazole, and *N*-methylimidazole. After comparing and examining the above conditions, we chose TBDPSCl as the silylation agent for introducing chromophore to **3** and using *N*-methylimidazole as the base with iodine as the catalyst to accelerate the reaction (89.1% yield).<sup>14</sup> Grignard reaction of **3** and (4-methylpentyl)magnesium bromide yielded the bulky side chain ketone **5** with 47.6% yield.

We designed the synthesis route by introducing a 5,7-diene to **5** under 1,3-dibromo-5,5-dimethylhydantoin (dibromantoin)/AIBN/TBAB/TBAF conditions; thus, the deprotection of silicon ether can be used in the same step under TBAF treatment. However, we found from TLC analysis that there was a more complex set of reaction products with silyl protected substrate compared with a similar reaction from acetyl protected substrate in the preparation of 20S(OH)-7DHC. Neither the dibromantoin condition nor the NBS/ $\gamma$ -collidine reaction afforded satisfactorily pure 5,7-diene product. Moreover, 5,7-diene structures are known to be unstable under light and acidic conditions. Thus, we chose to postpone the formation of the 5,7-diene and to replace TBDPS protection with acetyl protection. The deprotection of silicon ether with TBAF afforded the 3 $\beta$ -hydroxyl **6** in satisfactory yield (quantitative). Introducing the acetyl protecting group at 3 $\beta$ -OH with acetyl chloride and pyridine gave **7** in an 88.7% yield.

Transformation of **7** into the 5,7-diene **9** was carried out by dibromantoin/AIBN employed in the synthesis of 20S(OH)-7DHC using hexane and benzene as the solvent in the bromination step. Treatment of TBAB/TBAF in THF yielded the diene via dehydrobromination. The purification of the product **9** (34% overall yield) was carried out through silver nitrate impregnated silica gel chromatography to remove other impurities such as the 4,6-diene byproduct. Grignard reaction of 5,7-diene substrate **9** with CH<sub>3</sub>MgI afforded the precursor 20R(OH)-7DHC **10** (yield 85.6%).

**Scheme 1.** Chemical Synthesis of 20R(OH)D3



For B-ring-opening, 20R(OH)-7DHC **10** was subjected to UVB irradiation for 20 min in a quartz tube at 65 °C to achieve the maximum conversion to pre-20R(OH)D3 (**11**). The mixture was incubated at room temperature for 1 week, which produced a mixture of 20R(OH)D3 (**12**), 20R(OH)-tachysterol (**13**), 20R(OH)-lumisterol (**14**), and other minor 20R(OH) products. The photolysis reaction and subsequent time-dependent conversion to 20R(OH)D3 were analyzed by HPLC. The final 20R(OH)D3 was purified by a Gilson semipreparative HPLC system.

Different epimers of both 20(OH)-7DHC precursors and final 20-hydroxyvitamin D3 analogues have characteristic HPLC retention times ( $t_R$ ). The  $t_R$  of precursor 20R(OH)-7DHC appeared at 16.0 min, and its 20S counterpart could be eluted earlier at 13.8 min under the same HPLC conditions. The final 20R(OH)D3 showed a slight difference as compared to the 20S(OH)D3 isomer peak at  $t_R$  of 12.3 min vs 12.2 min, respectively (see Supporting Information).

$^1\text{H}$  NMR comparisons of both 20(OH)-7DHC epimer precursors and final 20(OH)D3 products are effective methods to identify 20R and 20S isomers of vitamin D3 analogues. It is established that in the pregnane compounds, the  $^1\text{H}$  NMR chemical shifts for the 21-Me in the 20S-OH isomers are downfield relative to 20R-OH isomers.<sup>12a</sup> They have distinct values and are the basis used to assign the absolute configuration at C<sub>20</sub> of these two epimers. The R-configuration at C<sub>20</sub> can be deduced from comparisons of  $^1\text{H}$  NMR spectra of 21-methyls in precursor 20R/S(OH)-7DHC and final 20R/S(OH)D3. An upfield chemical shift (1.16 ppm) was obtained for the 21-methyl in 20R(OH)-7DHC, while in 20S(OH)-7DHC a downfield chemical shift at 1.27 ppm was observed. Similarly, we found that the 21-Me showed a chemical shift at 1.13 ppm in 20R-isomer of 20(OH)D3 while a downfield chemical shift of 1.24 ppm was observed for 21-Me in 20S(OH)D3 (as shown in Figure 3,  $^1\text{H}$  NMR spectra of 20R/S(OH)-7DHC are shown in Supporting Information).

**Biological Evaluations.** Previously we documented that 20S(OH)D3 and related 20S(OH)D2 inhibit proliferation and stimulate differentiation of human epidermal keratinocytes (HEKn) in a dose dependent manner similar to 1,25(OH)<sub>2</sub>D3

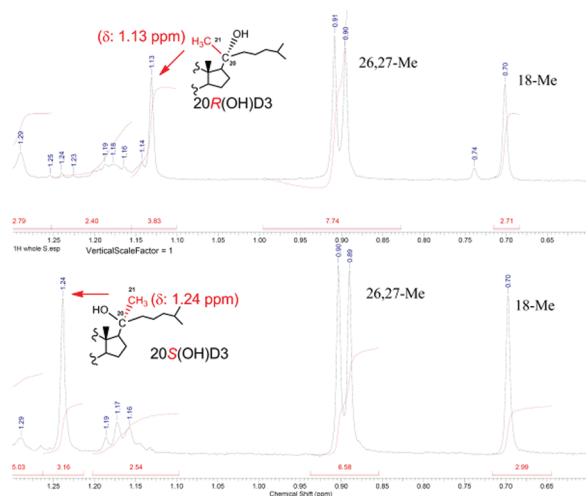


**Figure 3.** Comparison of  $^1\text{H}$  NMR chemical shifts for 21-Me in 20R and 20S(OH)D3. 21-Me showed a chemical shift at 1.13 ppm in 20R(OH)D3, while the downfield chemical shift of 1.24 ppm was observed for 21-Me in 20S(OH)D3.

with the highest potency at  $>10^{-10}$  M.<sup>6b,8b,15</sup> In the present study we compared the antiproliferative activity of 20S(OH)D3 with its epimer 20R(OH)D3. Figure 4 shows that 20S(OH)D3

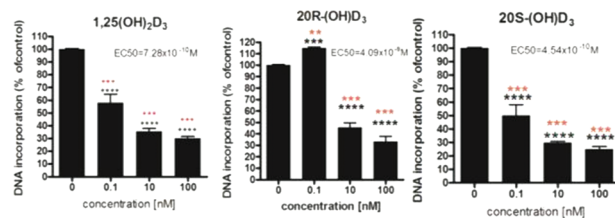


**Figure 4.** 20(OH)D3 isomers inhibit growth of human keratinocytes. HEKn cells were treated for 24 h with 1,25(OH)<sub>2</sub>D3 or R or S epimers of 20(OH)D3 at the concentrations listed. The rate of  $^3\text{H}$ -thymidine incorporation into DNA served as a measure of proliferative activity. Data are presented as the mean  $\pm$  SD,  $n = 4$ . Incorporation into DNA is shown as percent (%) of control (ethanol treated cells). Statistical significance was measured using Student  $t$  test (\*) and one-way ANOVA (red asterisk) presented as (\*\*)  $p < 0.05$ , (\*\*\*)  $p < 0.01$ , and (\*\*\*\*)  $p < 0.001$ .

and 1,25(OH)<sub>2</sub>D3 (positive control) exhibited similar dose-dependent inhibition of proliferation, as expected, with an  $\text{EC}_{50}$  of  $7.28 \times 10^{-10}$  and  $4.54 \times 10^{-10}$  M, respectively. In contrast, 20R(OH)D3 had a biphasic effect, slightly stimulating DNA synthesis at 0.1 nM, with significant ( $p < 0.001$ ) inhibition of cell proliferation at  $\geq 10$  nM. This inhibitory effect was similar to that of 20S(OH)D3 ( $<50\%$  of control), however, with higher  $\text{EC}_{50}$  of  $4.09 \times 10^{-9}$  M. These data show a clear difference between the R and S isomers at low concentrations of the ligand (0.1 nM) and similar effects at the higher concentrations, however, with lower potency for the R form. In a separate experiment we demonstrated that 20S(OH)D3 and 1,25-(OH)<sub>2</sub>D3 inhibit colony formation by HaCaT epidermal keratinocytes with similar potency while 25(OH)D3 has no or a small effect (Supporting Information).

#### Metabolism of 20(OH)D3 by CYP11A1 and CYP27B1.

Since biologically generated 20S(OH)D3 is derived from the action of P450scc on vitamin D3 and can be further metabolized to dihydroxy (e.g., 17,20(OH)<sub>2</sub>D3, 20,22-(OH)<sub>2</sub>D3, 20,23(OH)<sub>2</sub>D3) and trihydroxy (e.g., 17,20,23-(OH)<sub>3</sub>, 20,22,X(OH)<sub>3</sub>D3) metabolites by this enzyme,<sup>6a,7,16</sup> we compared the ability of P450scc to metabolize 20S(OH)D3 and 20R(OH)D3 (Figure 5A). Because of the formation of many products, metabolites were characterized in the case of the 20S-isomer<sup>16</sup> but not for the 20R-isomer; data are presented as the amount of substrate metabolized. 20R(OH)D3 proved to be a much better substrate than 20S(OH)D3 for P450scc with 58% being consumed in the first 2 min of incubation for the R-isomer but only 13% for the S-isomer. While the structures of the products from 20R(OH)D3 remain to be elucidated, HPLC retention times are consistent with formation of di- and trihydroxy derivatives analogous to those produced from the 20S-isomer.<sup>16</sup>

CYP27B1 catalyzes the  $1\alpha$ -hydroxylation of a range of vitamin D derivatives including 20(OH)D3 and 20(OH)-D2.<sup>15,17</sup> In the case of 20S(OH)D3, the  $1\alpha,20\text{S}$ -dihydroxyvitamin D3 product exhibits calcemic activity which is in contrast to the parent 20S(OH)D3 which lacks this activity.<sup>8a</sup> We therefore compared the ability of CYP27B1 to metabolize 20S(OH)D3 and 20R(OH)D3 (Figure 5B). Each isomer was metabolized to a single product at comparable initial rates, but subsequently the rate declined more rapidly for the R-isomer

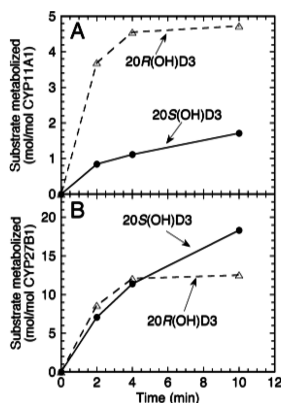


**Figure 5.** Metabolism of 20(OH)D3 isomers by CYP11A1 and CYP27B1. Substrates were incorporated into phospholipid vesicle and incubated with CYP11A1 (A) or CYP27B1 (B) and then substrate and products extracted with dichloromethane and analyzed by reverse phase HPLC.

than the *S*-isomer. This phenomenon could suggest that the 20R(OH)D3 isomer could show less calcemic toxicity than 20S(OH)D3 because of its lower efficiency of 1 $\alpha$ -hydroxylation. The hypercalcemic effects of the 1 $\alpha$ -hydroxy metabolites will be examined in future studies.

## CONCLUSION

We chemically synthesized the *R* epimer of 20(OH)D3 based on the preferred conformation of the reactant and the associated strong steric preference for the formation of this isomer. NMR characterization of the chemically synthesized compound and comparisons with 20S(OH)-7DHC and 20S(OH)D3 confirmed the *R* chirality at the C20 position. Biological studies demonstrated the antiproliferative activity of *R*-epimer on keratinocytes, similar to that of the *S*-epimer and 1,25(OH)<sub>2</sub>D3 at 10 and 100 nM, with a noted difference (opposite effect) at lower concentrations. This overlapping but different behavior was further demonstrated by the ability of P450<sub>sc</sub> and CYP27B1 to metabolize the *R* and *S* epimers but with the different efficiencies. 20R(OH)D3 was a better substrate for P450<sub>sc</sub> than 20S(OH)D3, while 20S(OH)D3 was a better substrate for CYP27B1 than for 20R(OH)D3. The latter could explain the higher potency of 20S(OH)D3 in the inhibition of HEK cell proliferation. Alternatively, P450<sub>sc</sub>, which is present in keratinocytes,<sup>18</sup> may cause a more rapid inactivation of the *R*-epimer than the *S*-epimer; however it remains to be established if the products of P450<sub>sc</sub> action on 20R(OH)D3 are more or less potent than the parent compound. In depth investigations of the biological activity of 20R/S(OH)D3 epimers for anti-inflammatory and hypercalcemic effects, the nature of signal transduction pathways induced by these compounds, and the potential role of 1-hydroxylation in these processes will be carried out in the future.

## EXPERIMENTAL PROCEDURES

All reagents for the synthesis were purchased from commercial sources and were used without further purification. Moisture-sensitive reactions were carried out under an argon atmosphere. NMR spectra were obtained on a Bruker ARX 300 MHz (Billerica, MA) or an Agilent Inova 500 MHz spectrometer (Santa Clara, CA). Mass spectral data were collected on a Bruker ESQUIRE-LC/MS system equipped with an ESI source. High resolution mass spectra were recorded on a

Waters Xevo G2 QTOF LCMS using ESI. The purity of the final compounds was analyzed by an Agilent 1100 HPLC system (Santa Clara, CA). Purities of the compounds were established by careful integration of areas for all peaks detected and  $\geq 95\%$ .

(1*S*,*Z*)-3-((*E*)-2-((7 $\alpha$ *S*)-1-((*R*)-2-Hydroxy-6-methylheptan-2-yl)-7 $\alpha$ -methylhexahydro-1*H*-inden-4(2*H*)-ylidene)ethylidene)-4-methylenecyclohexanol (20R(OH)D3, **12**). A methanol solution of 20R(OH)-7DHC (**10**) (5 mg, 2 mg/mL) was subjected to UVB irradiation for 20 min in a quartz tube at 65 °C, using a Rayonet RPR-100 photochemical reactor (Branford, CT). The mixture was incubated at room temperature for 1 week to allow the conversion from pre-20R(OH)D3 (**11**) to 20R(OH)D3 (**12**). The mixture was analyzed using an Agilent 1100 HPLC system (Santa Clara, CA) to confirm the production of 20R(OH)D3 and to optimize the conditions for the separation using a semipreparative HPLC system. The reaction mixture (5  $\mu$ L) of irradiated 20R(OH)-7DHC was injected by an autosampler onto a 5  $\mu$ m Phenomenex Luna-PFP column (250 mm  $\times$  4.6 mm) (Torrance, CA) with mobile phase of 85% methanol–water at a flow rate of 1.0 mL/min. The separation of the mixture was conducted using a Gilson semipreparative HPLC system with a 5  $\mu$ m Phenomenex Luna-PFP semipreparative column (250 mm  $\times$  10 mm) and a mobile phase as 85% methanol–water at a flow rate of 6.0 mL/min. Fractions were collected based on a preset UV threshold and were reanalyzed by RP-HPLC. Fractions containing above 95% of pure **12** (for 240 and 265 nm spectra) were pooled, freeze-dried, and characterized by NMR and MS. <sup>1</sup>H NMR (500 MHz, MeOH-*d*<sub>4</sub>):  $\delta$  6.22 (d, 1 H, *J* = 10.0 Hz), 6.02 (d, 1 H, *J* = 10.0 Hz), 5.04 (s, 1 H), 4.74 (s, 1 H), 3.78–3.74 (m, 1 H), 2.87–2.84 (m, 1 H), 2.54–2.52 (m, 1 H), 2.42–2.39 (m, 1 H), 2.21–2.09 (m, 2 H), 2.01–1.96 (m, 1 H), 1.74–1.14 (m, 26 H), 1.13 (s, 3 H), 0.91 (d, 6 H, *J* = 5.0 Hz), 0.71 (s, 3 H). MS (ESI) *m/z* 423.4 [M + Na]<sup>+</sup>. HPLC purity 100%. HRMS calculated for C<sub>27</sub>H<sub>45</sub>O<sub>2</sub> [M + H]<sup>+</sup> 401.3420. Found 401.3423.

**Metabolic Studies of 20(OH)D3.** To test enzymatic metabolism, the 20S(OH)D3 and 20R(OH)D3 substrates were incorporated into phospholipid vesicles prepared from dioleoylphosphatidylcholine and cardiolipin as before,<sup>19</sup> with the ratio of substrate to phospholipid being 0.025 mol/mol phospholipid. Vesicles were incubated with 2  $\mu$ M bovine CYP11A1 or 0.06  $\mu$ M human CYP27B1 at 37 °C for up to 10 min. Products and remaining substrate were extracted with dichloromethane and measured by reverse phase HPLC as described before.<sup>16,17b</sup>

**Inhibition of Proliferation by Different Epimers of 20(OH)D3 in Comparison to Calcitriol.** Neonatal human epidermal keratinocytes (HEK<sub>n</sub>) were isolated from neonatal foreskin of African-American donors and grown in HKM (Lonza) medium supplemented with HKGF (Lonza) as described previously.<sup>8b,c</sup> For the cell proliferation assay the cells from a third passage were seeded into 24-well plates (TPP, Switzerland) and grown to  $\sim 80\%$  confluence. Secosteroids were dissolved in ethanol and then diluted in keratinocyte medium containing 0.1% BSA (Sigma). Cells were incubated for 24 h. Then 1  $\mu$ Ci/ml [<sup>3</sup>H]thymidine (Moravsek Biochemicals Inc., Brea, CA) was added and cells were incubated for a further 4 h. Excess of unbound thymidine was removed by washing cells with PBS. Cells were precipitated with 10% trichloroacetic acid (TCA) (Sigma) and then the precipitate was dissolved with 1 N NaOH. The solution was collected in vials, and thymidine incorporation was determined using a liquid scintillation counter (Beckman LS 6000, Santa Clara, CA).

## ASSOCIATED CONTENT

### Supporting Information

Preparations and spectra of intermediates. This material is available free of charge via the Internet at <http://pubs.acs.org>.

## AUTHOR INFORMATION

### Corresponding Author

\*For W.L.: phone, (901) 448-7532; e-mail, [wli@uthsc.edu](mailto:wli@uthsc.edu). For D.D.M.: phone, (901) 448-6026; e-mail, [dmiller@uthsc.edu](mailto:dmiller@uthsc.edu).

## Notes

The authors declare no competing financial interest.

## ACKNOWLEDGMENTS

The authors thank College of Pharmacy of UTHSC; the Van Vleet Endowed Professorship, UT Research Foundation, University of Western Australia; and NIH/NIAMS Grants R01AR052190 and 1R01AR056666-01A2 to A.T.S. for financial support. We thank Jerrod Scarborough for performing HRMS experiments.

## ABBREVIATIONS USED

D3, vitamin D3; 7-DHC, 7-dehydrocholesterol; 1,25(OH)<sub>2</sub>D3, 1 $\alpha$ ,25-dihydroxyvitamin D3; VDR, vitamin D receptor; P450<sub>sc</sub>, CYP11A1; HBTU, *O*-benzotriazole-*N,N,N',N'*-tetramethyluronium hexafluorophosphate; TMSCl, trimethylsilyl chloride; DIPEA, *N,N*-diisopropylethylamine; TBDMSCl, *tert*-butyldimethylsilyl chloride; AIBN, 2,2'-azobisisobutyronitrile; TBAF, tetrabutylammonium fluoride; TBDPSCl, *tert*-butylchlorodiphenylsilane

## REFERENCES

- (1) Plum, L. A.; DeLuca, H. F. Vitamin D, disease and therapeutic opportunities. *Nat. Rev. Drug Discovery* **2010**, *9* (12), 941–955.
- (2) Lappe, J. M. The role of vitamin D in human health: a paradigm shift. *J. Evidence-Based Complementary Altern. Med.* **2011**, *16*, 58–72.
- (3) (a) DeLuca, H. F. Overview of general physiologic features and functions of vitamin D. *Am. J. Clin. Nutr.* **2004**, *80* (6, Suppl.), 1689S–16896S. (b) Holick, M. F. Vitamin D Deficiency. *N. Engl. J. Med.* **2007**, *357*, 266–281.
- (4) Bouillon, R.; Okamura, W. H.; Norman, A. W. Structure–function relationships in the vitamin D endocrine system. *Endocr. Rev.* **1995**, *16* (2), 200–257.
- (5) (a) Pinette, K. V.; Yee, Y. K.; Amegadzie, B. Y.; Nagpal, S. Vitamin D receptor as a drug discovery target. *Mini-Rev. Med. Chem.* **2003**, *3* (3), 193–204. (b) Takahashi, T.; Morikawa, K. Vitamin D receptor agonists: opportunities and challenges in drug discovery. *Curr. Top. Med. Chem.* **2006**, *6* (12), 1303–1316. (c) Schwartz, G. G. Vitamin D and intervention trials in prostate cancer: from theory to therapy. *Ann. Epidemiol.* **2009**, *19* (2), 96–102.
- (6) (a) Slominski, A.; Semak, I.; Zjawiony, J.; Wortsman, J.; Li, W.; Szczesniowski, A.; Tuckey, R. C. The cytochrome P450<sub>sc</sub> system opens an alternate pathway of vitamin D3 metabolism. *FEBS J.* **2005**, *272* (16), 4080–4090. (b) Li, W.; Chen, J.; Janjetovic, Z.; Kim, T. K.; Sweatman, T.; Lu, Y.; Zjawiony, J.; Tuckey, R. C.; Miller, D.; Slominski, A. Chemical synthesis of 20S-hydroxyvitamin D3, which shows antiproliferative activity. *Steroids* **2010**, *75* (12), 926–935.
- (7) (a) Guryev, O.; Carvalho, R. A.; Usanov, S.; Gilep, A.; Estabrook, R. W. A pathway for the metabolism of vitamin D3: unique hydroxylated metabolites formed during catalysis with cytochrome P450<sub>sc</sub> (CYP11A1). *Proc. Natl. Acad. Sci. U.S.A.* **2003**, *100* (25), 14754–14759. (b) Tuckey, R. C.; Li, W.; Zjawiony, J. K.; Zmijewski, M. A.; Nguyen, M. N.; Sweatman, T.; Miller, D.; Slominski, A. Pathways and products for the metabolism of vitamin D3 by cytochrome P450<sub>sc</sub>. *FEBS J.* **2008**, *275* (10), 2585–2596.
- (8) (a) Slominski, A. T.; Janjetovic, Z.; Fuller, B. E.; Zmijewski, M. A.; Tuckey, R. C.; Nguyen, M. N.; Sweatman, T.; Li, W.; Zjawiony, J.; Miller, D.; Chen, T. C.; Lozanski, G.; Holick, M. F. Products of vitamin D3 or 7-dehydrocholesterol metabolism by cytochrome P450<sub>sc</sub> show anti-leukemia effects, having low or absent calcemic activity. *PLoS One* **2010**, *5* (3), e9907. (b) Zbytek, B.; Janjetovic, Z.; Tuckey, R. C.; Zmijewski, M. A.; Sweatman, T. W.; Jones, E.; Nguyen, M. N.; Slominski, A. T. 20-Hydroxyvitamin D3, a product of vitamin D3 hydroxylation by cytochrome P450<sub>sc</sub>, stimulates keratinocyte differentiation. *J. Invest. Dermatol.* **2008**, *128* (9), 2271–2780. (c) Janjetovic, Z.; Zmijewski, M. A.; Tuckey, R. C.; DeLeon, D. A.; Nguyen, M. N.; Pfeffer, L. M.; Slominski, A. T. 20-Hydroxycholecalciferol, product of vitamin D3 hydroxylation by P450<sub>sc</sub>, decreases NF-kappaB activity by increasing IkappaB alpha levels in human keratinocytes. *PLoS One* **2009**, *4* (6), e5988.
- (9) Tocchini-Valentini, G.; Rochel, N.; Wurtz, J. M.; Mitschler, A.; Moras, D. Crystal structures of the vitamin D receptor complexed to superagonist 20-epi ligands. *Proc. Natl. Acad. Sci. U.S.A.* **2001**, *98* (10), 5491–5496.
- (10) (a) Liu, Y. Y.; Collins, E. D.; Norman, A. W.; Peleg, S. Differential interaction of 1 $\alpha$ ,25-dihydroxyvitamin D3 analogues and their 20-epi homologues with the vitamin D receptor. *J. Biol. Chem.* **1997**, *272* (6), 3336–3345. (b) Yang, W.; Freedman, L. P. 20-Epi analogues of 1,25-dihydroxyvitamin D3 are highly potent inducers of DRIP coactivator complex binding to the vitamin D3 receptor. *J. Biol. Chem.* **1999**, *274* (24), 16838–16845.
- (11) Hansen, K. B.; Claus Aage, S. Vitamin D Analogues Containing a Hydroxy Group in the 20-Position. U.S. Patent US 5589471, 1996.
- (12) (a) Mijares, A.; Cargill, D. I.; Glasel, J. A.; Lieberman, S. Studies on the C-20 epimers of 20-hydroxycholesterol. *J. Org. Chem.* **1967**, *32* (3), 810–812. (b) Nes, W. R.; Varkey, T. E. Conformational analysis of the 17(20) bond of 20-keto steroids. *J. Org. Chem.* **1976**, *41* (9), 1652–1653. (c) Komori, M. H. T. Structures of thornasterols A and B (biologically active glycosides from asteroidia, XI). *Tetrahedron Lett.* **1986**, *27* (29), 3369–3372.
- (13) Djerassi, C.; Staunton, J. Optical Rotatory Dispersion Studies. XLI.  $\alpha$ -Haloketones (Part 9). Bromination of Optically Active *cis*-1-Decalone. Demonstration of Conformational Mobility by Rotatory Dispersion. *J. Am. Chem. Soc.* **1961**, *83*, 736–743.
- (14) Bartoszewicz, A.; Marcin, K.; Stawinski, J. Iodine-promoted silylation of alcohols with silyl chlorides. Synthetic and mechanistic studies. *Tetrahedron* **2008**, *64* (37), 8843–8850.
- (15) Slominski, A. T.; Kim, T. K.; Janjetovic, Z.; Tuckey, R. C.; Bieniek, R.; Yue, J.; Li, W.; Chen, J.; Nguyen, M. N.; Tang, E. K.; Miller, D.; Chen, T. C.; Holick, M. 20-Hydroxyvitamin D2 is a noncalcemic analog of vitamin D with potent antiproliferative and prodifferentiation activities in normal and malignant cells. *Am. J. Physiol.: Cell Physiol.* **2011**, *300* (3), C526–C541.
- (16) Tuckey, R. C.; Li, W.; Shehabi, H. Z.; Janjetovic, Z.; Nguyen, M. N.; Kim, T. K.; Chen, J.; Howell, D. E.; Benson, H. A.; Sweatman, T.; Baldisseri, D. M.; Slominski, A. Production of 22-hydroxy metabolites of vitamin D3 by cytochrome P450<sub>sc</sub> (CYP11A1) and analysis of their biological activities on skin cells. *Drug Metab. Dispos.* **2011**, *39* (9), 1577–1588.
- (17) (a) Tang, E. K.; Li, W.; Janjetovic, Z.; Nguyen, M. N.; Wang, Z.; Slominski, A.; Tuckey, R. C. Purified mouse CYP27B1 can hydroxylate 20,23-dihydroxyvitamin D3, producing 1 $\alpha$ ,20,23-trihydroxyvitamin D3, which has altered biological activity. *Drug Metab. Dispos.* **2010**, *38* (9), 1553–1559. (b) Tang, E. K.; Voo, K. J.; Nguyen, M. N.; Tuckey, R. C. Metabolism of substrates incorporated into phospholipid vesicles by mouse 25-hydroxyvitamin D3 1 $\alpha$ -hydroxylase (CYP27B1). *J. Steroid Biochem. Mol. Biol.* **2010**, *119* (3–5), 171–179.
- (18) Slominski, A.; Zjawiony, J.; Wortsman, J.; Semak, I.; Stewart, J.; Pisarchik, A.; Sweatman, T.; Marcos, J.; Dunbar, C.; Tuckey, R. C. A novel pathway for sequential transformation of 7-dehydrocholesterol and expression of the P450<sub>sc</sub> system in mammalian skin. *Eur. J. Biochem.* **2004**, *271* (21), 4178–4188.
- (19) Tuckey, R. C.; Nguyen, M. N.; Slominski, A. Kinetics of vitamin D3 metabolism by cytochrome P450<sub>sc</sub> (CYP11A1) in phospholipid vesicles and cyclodextrin. *Int. J. Biochem. Cell Biol.* **2008**, *40* (11), 2619–2626.